## Symbols and Commonly Used Constants

**Symbols**

$C_s$ = ion sound speed $\approx \sqrt{\frac{KT_e}{M}}$

E = particle kinetic energy

$E_b$ = beam energy

$I_{es}$, $I_{is}$ = electron, ion saturation current

K = Boltzmann's constant

M, $m_i$ = ionic mass

$T_b$ = ion beam temperature equivalent

$T_e$, $T_i$ = electron, ion temperature

$V_d$ = discharge potential

$V_g$ = grid potential

$V_f$ = floating potential

$V_s$ = plasma space potential

$a_e$ = electron thermal speed = $\sqrt{\frac{KT_e}{m}}$

$a_i$ = ion thermal speed = $\sqrt{\frac{KT_i}{M}}$

e = electronic charge

$f_b(v)$ = beam ion velocity distribution

$f_e(v)$, $f_i(v)$ = electron, ion velocity distribution functions

k = wavenumber

m, $m_e$ = electronic mass

n, $n_i$ = electron density, ion density

$n_b$ = beam density

$v_B$ = Bohm (Tonks-Langmuir) speed = $\sqrt{\frac{KT_e}{M}}$

$v_b$ = beam velocity

$v_e$ = average magnitude of electron velocity (3 dim) = $\sqrt{\frac{8KT_e}{m}}$

$v_g$ = group velocity

$v_p$ = phase velocity

$z_o$ = axial plasma position

$\lambda_D$, $\lambda_{De}$ = electron Debye length $= \sqrt{\frac{\gamma K T_e}{4\pi n e^2}}$

$\theta$ = ion/electron temperature ratio $= \frac{T_i}{T_e}$

$\omega$ = frequency

$\omega_p$, $\omega_{pe}$ = electron plasma frequency $= \sqrt{\frac{4\pi n e^2}{m}}$

$\omega_{pi}$ = ion plasma frequency $= \sqrt{\frac{4\pi n e^2}{M}}$

$\tilde{\omega}$ = normalized wave frequency $= \frac{\omega}{\omega_{pi}}$

$\sigma_c$ = charge exchange cross sections, e.g., $\sigma_{Ar^+ - Ar} \sim 5 \times 10^{-15}$ cm$^2$

(velocity dependent)

Physical Constants (CGS)

| | |
|---|---|
| Boltzmann's constant | $K = 1.3807 \times 10^{-16}$ erg/°K |
| Elementary charge | $e = 4.8032 \times 10^{-10}$ statcoulomb |
| Electronic mass | $m = 9.1095 \times 10^{-28}$ gram |
| Hydrogen atom mass | $M_p = 1.6734 \times 10^{-24}$ gram |
| Speed of light in vacuum | $c = 2.9979 \times 10^{10}$ cm/sec |

Temperature associated with 1 eV = $1.1605 \times 10^4$ °K

Atomic Masses for Typical Plasma Gases

| Gas | Mass (AMU) |
|---|---|
| He | 4.0026 |
| Ne | 19.9924 |
| Ar | 39.9624 |
| Kr | 83.9115 |
| Xe | 130.905 |

# Chapter I. Plasma Production

A plasma source which possesses the desirable characteristics of quiescence and uniformity has been developed at the UCLA Plasma Physics Laboratory and is now being used in many parts of the world for basic plasma research. Because this source is economical to build and simple to operate, it is ideally suited to the undergraduate or graduate plasma laboratory. All the experiments to be described in this text can be performed in this one device.

## 1) The D.C. Discharge

Plasma can be produced by electron bombardment of a neutral gas in an otherwise evacuated vessel. In the D.C. discharge, a current is passed through a set of filaments (tantalum or thoriated tungsten wire) to heat them by joule heating. A significant number of electrons in the hot filament can have an energy greater than the work function and are emitted. These electrons, called primary electrons, are accelerated by an external D.C. electric field such that they have sufficient energy to ionize the neutral gas. The minimum energy required to remove the first valence electron from the neutral atom (the first ionization energy) is in the neighborhood of 20 eV for commonly used gases at room temperature. A discharge potential above this energy must be applied between the filaments (cathode) and the chamber wall (anode) to obtain a discharge. The removed valence electron is called a secondary electron and is scattered with less energy than the corresponding incident primary electron; at any given time most electrons in the plasma are secondaries.

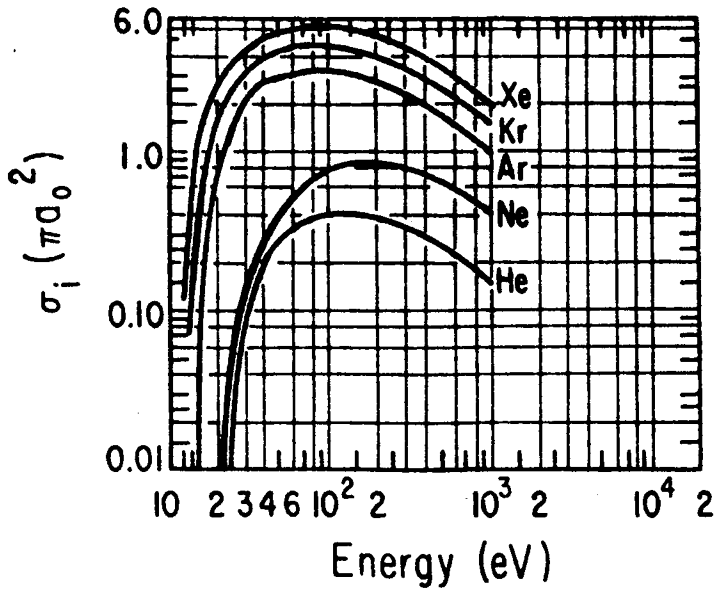


Figure I-1.

Ionization cross sections for Xe, Kr, A, Ne and He by electron impact.

$\pi a_o^2$ = cross section of H atom = $8.8 \times 10^{-17}$ cm$^2$

The probability of an ionizing collision (ionization cross section) generally has a broad maximum for electrons with energy about 100 eV as seen in Figure I-1. The D.C. discharge is typically operated with a potential of 30 to 100 volts between the cathode and the anode wall. Doubly ionizing collisions can also occur when the primary electrons' energy exceeds the second ionization energy; however, the ionization cross section for double ionization is usually much smaller than for single ionizations. The first and the second ionization energies of several commonly used gases are listed in Table I-1. Schematic diagram of the D.C. discharge system is shown in Figure I-2.

a) Space charge limited emission: In the presence of an insignificant number of neutral atoms (as in a vacuum tube) only a small current can flow between the cathode and the anode. This current limiting is the result of space charge due to electrons which accumulate near the cathode and repel some of the newly emitted electrons. The space charge limited emission current is given by the Child-Langmuir law[1] $J = 2.33 \times 10^{-6} \times \cdot \left(\frac{V_d{}^{3/2}}{d^2}\right)$ A/cm$^2$, where $V_d$ is the discharge potential in volts and d is the distance between anode and cathode in cm. For instance, for d = 15 cm, $V_d = 40$ V, $J = 2.6 \times 10^{-6}$ A/cm$^2$.

b) Temperature limited emission: In a plasma device, the initially small space charge limited discharge current ionizes some neutrals. The ions produced partially neutralize the space charge allowing a larger discharge current which produces more plasma. Eventually a sheath is formed around the cathode making the plasma the effective anode. This reduces d to a few Debye lengths. For $n = 10^{10}$ cm$^{-3}$ and $T_e = 3$ eV, the Debye length

TABLE I-1

| GAS | FIRST IONIZATION LEVEL (eV) | SECOND IONIZATION LEVEL (eV) |
|---|---|---|
| H | 13.595 | ------- |
| He | 24.481 | 54.403 |
| Ne | 21.559 | 41.07 |
| Ar | 15.755 | 27.62 |
| Kr | 13.9 | 26.4 |
| Xe | 12.127 | 21.2 |

Source: CRC Handbook of Chemistry and Physics, 1967 Edition (Page E-56).

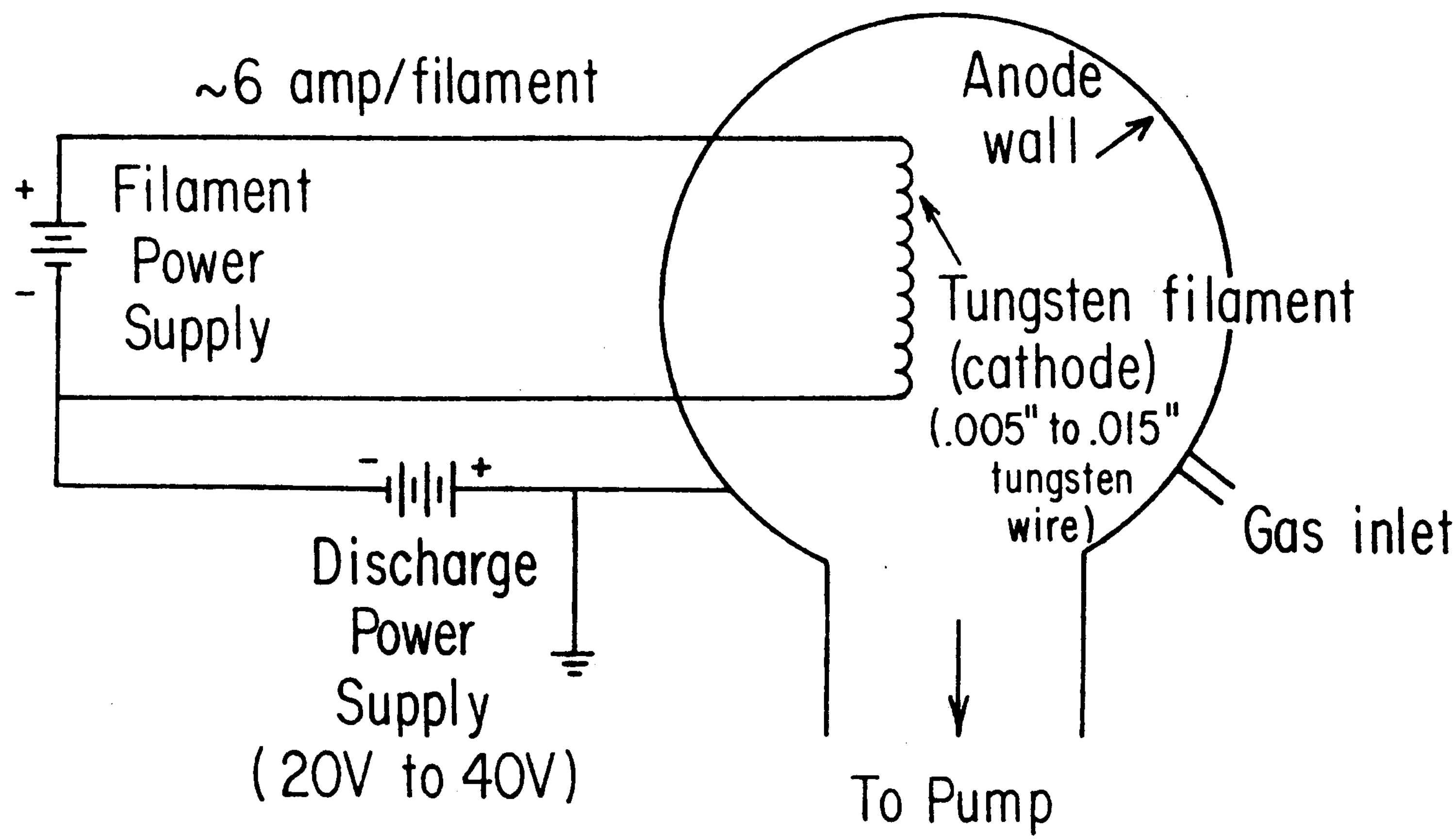


Figure I-2.

Discharge Diagram

is about $10^{-2}$ cm and the space charge limiting current density, $J = 5.9\ A/cm^2$.

The total emission current is, however, limited by the filament temperature. The temperature limited emission current is given by the Richardson law: $J = AT^2e^{-W/KT}\ A/cm^2$ where W and T are the work function and temperature respectively of the filament metal. The theoretical limit for A is $4\pi meK^2/h^3 = 120\ A/cm^2 - K^{\circ 2}$. In actual practice, A varies from 30 - 200 $A/cm^2 - K^{\circ 2}$. For tungsten, $W \simeq 4.5$ eV, $A = 60\ A/cm^2 - K^{\circ 2}$, and the melting temperature is 3650° K. The Richardson law gives for tungsten at 2000° K, $J = 1.1 \times 10^{-3}$ $A/cm^2$.

Comparison of the temperature and space charge limiting processes shows that in the presence of the plasma, $J_{\text{space charge}} >> J_{\text{temperature}}$. The discharge current, which is just the emission current, is, then, a sensitive function of the filament temperature.

One method of producing a high % ionization is to heat the filaments to a high temperature (white hot at 3000° K) by high current pulses (50 amps for a filament of .030" diameter, 3" length). In this manner, plasma densities exceeding $10^{12}$ $cm^{-3}$ can be achieved while preserving filament life span.

c) Balance between production and losses: The plasma production and losses can be represented by the following rate equation:

$$\frac{\partial N}{\partial t} = \left(\frac{\partial N}{\partial t}\right)_{\text{production}} - \left(\frac{\partial N}{\partial t}\right)_{\text{loss}}$$

In the steady-state, we have

$$\left(\frac{\partial N}{\partial t}\right)_{\text{production}} = \left(\frac{\partial N}{\partial t}\right)_{\text{loss}}$$

where N is the total number of plasma particles (electron-ion pair) in the system. Let $\sigma$ represent the ionization cross-section of the neutral gas to be ionized by electrons of energy $eV_d$; $n_\circ$ the density of neutrals; $\ell_{eff}$ the average total distance a primary electron travels before it is lost from the plasma (effective path length); $n_e v_d$ the primary electron flux through a surface of area A enclosing the filaments; and $\lambda = \frac{1}{n_\circ \sigma}$ the ionizing collision mean free path for primary electrons. Then, in the D.C. discharge

$$\left(\frac{\partial N}{\partial t}\right)_{production} = n_\circ \sigma \ell_{eff} \, (n_e v_d A) = n_\circ \sigma \ell_{eff} \, \frac{I_{discharge}}{e} \tag{I-1}$$

in the limit $\lambda >> \ell_{eff}$. For simplicity, imagine a primary electron discharge surface of area A as

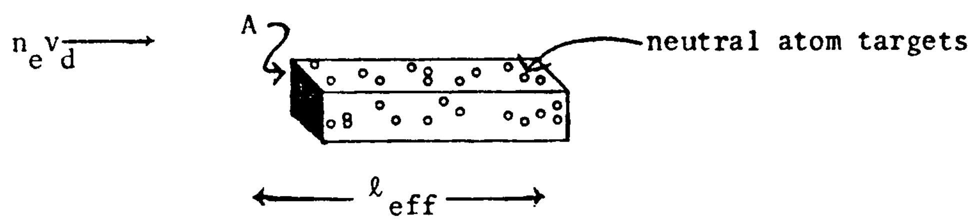


the end of a cylinder of length $\ell_{eff}$ filled with neutral targets, recognizing the product $(n_e)(\ell_{eff}A)$ above as the number of primary electrons per unit volume times the total volume of neutral atom targets accessible to the primaries. We can now understand (I-1) by rearranging it as

$$\left(\frac{\partial N}{\partial t}\right)_{production} = (n_e \ell_{eff} A)(n_\circ \sigma v_d),$$

and identify $n_e \ell_{eff} A$ as the total number of ionizing primary electrons available within the plasma volume at any given instant of time and $n_\circ \sigma v_d$ as the rate of ionizing collisions by a single primary electron. The limit $\lambda = \frac{1}{n_\circ \sigma} >> \ell_{eff}$ states that the ionization mean free path is sufficiently long such that the primary electrons are uniformly distributed inside the plasma volume. Under this condition of uniform probability of plasma production over the entire volume equation (I-1) is valid.

There are generally three types of major losses of plasma particles.

1. Loss to the chamber wall.

2. Volume recombination - secondary electrons engage in low velocity collisions with ions to produce neutrals.

3. Loss to probes, filament supports, any other obstacles, insulators or conductors which become plasma sinks through surface recombination. The total plasma loss can be expressed by

$$\left(\frac{\partial N}{\partial t}\right)_{loss} \simeq \frac{nV}{\tau}$$

where V is the volume of the system, n is the plasma density and $\tau$ is the plasma lifetime. In a system where ions can flow to the chamber wall freely, the plasma lifetime is $\tau = \frac{L}{v_i}$, where $v_i$ is the flow velocity of ions and L is the scale length of the system. Using this expression, we obtain

$$\left(\frac{\partial N}{\partial t}\right)_{loss} \simeq n\, v_i\, A$$

where A is the total plasma surface area.

3) Experimental Procedure

a) General familiarization: Leak in enough Argon to raise the neutral pressure to about $3 \times 10^{-3}$ torr and turn the filament power supply to a minimum voltage with the switch off. Then the switch is turned on, and the filament voltage is carefully turned up until the cathode wires glow red hot. The discharge power supply is set to the desired value (about 50 V) and then the filament voltage is turned up until the desired discharge current ($I_d$) is obtained ~500 MA. Notice that as the filament voltage is turned up, the discharge current increases rapidly (emission limited current flow). Be very careful in the adjustment of the filament voltage, since when the filament is hot enough to emit electrons, it is on the verge of melting. The filament biased negatively with respect to the plasma is slowly destroyed by ion bombardment and must be replaced periodically. The filament life span will be shortened if it is subjected to a large surge of current. Thus, always vary the filament voltage slowly until the discharge current is obtained. The neutral gas pressure can be read off an ionization gauge. Pressure adjustments are made with a leak valve. Some typical operating conditions are listed in Appendix B.

b) Saturation ion current measurement:

Set up a negative bias -100 Volts circuit to obtain the ion saturation current, $I_{is}$. Check to see that current is positive (if not, increase bias). Compute the ratio $I_{es}/I_{is}$. Does this ratio depend on the plasma density? How should this ratio depend on ion mass?

---

* The factor $\frac{1}{4}$ arises from the following:

$\frac{1}{2}$ - due to plasma at edge of sheath surrounding probe being composed of particles with velocity $0 \rightarrow \infty$ toward probe face only.

$\frac{1}{2}$ - due to average of direction cosine over hemisphere since particles may strike probe at angles $0 < \theta < \pi$ to the probe plane.

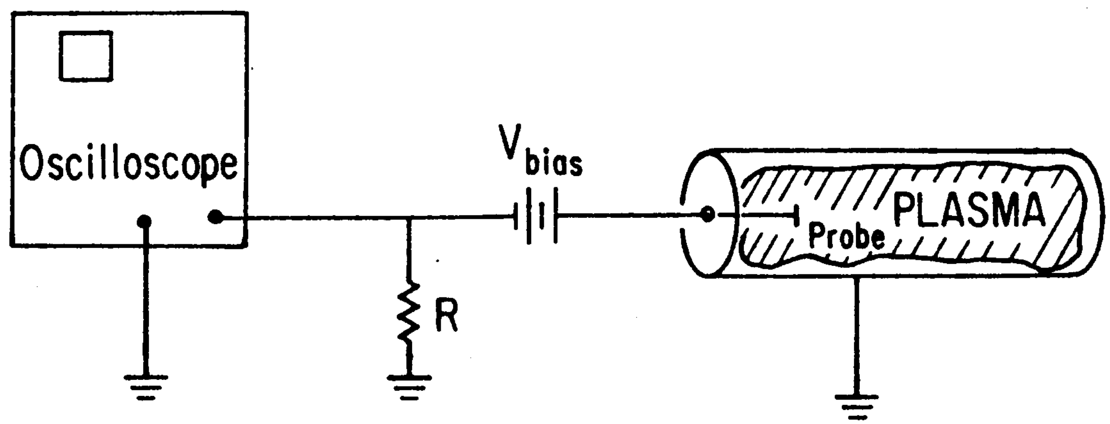


Figure I-5.

c) Dependence of plasma parameters on external parameters: Measure the ~~electron~~ ion saturation current as a function of:

1. Discharge voltage (with chosen neutral pressure and filament current).

2. Discharge current (with chosen discharge voltage and neutral pressure). This is adjusted by varying the filament current. Be careful not to turn the filament current up too high and destroy the filaments.

3. Neutral pressure ($10^{-5}$ - $10^{-3}$ torr, at fixed discharge and filament currents).

To make the results of these measurements more accurate, the electron saturation current and the electron temperature should be measured by displaying the full Langmuir probe trace on an oscilloscope. The student should look ahead to Chapter II, pages 43 - 49 for an explanation of the Langmuir probe method.

Determine the dependence of plasma density on the discharge voltage. How does this dependence relate to the variation of ionization cross section with electron energy (Figure I-1)? Compute the fractional ionization, $n/n_{neutral}$ for at least three different pressure settings. Does the fractional ionization remain constant for a constant discharge current?

d) Plasma lifetime measurement: A flat stainless steel plate is placed in the magnetic field-free region and biased at -75 volts with respect to the anode. This induces additional ion loss such that in the steady state, the balance equation becomes

$$\left(\frac{\partial N}{\partial t}\right)_{production} = \frac{n_1 V}{\tau} + \frac{I_i}{e}$$

where $n_1$ is the plasma density when there is an ion current $I_i$ extracted by the plate. The plasma production rate may be expressed in terms of the discharge current $I_d$ and the effective electron path length $\ell_{eff}$ as

$$\left(\frac{\partial N}{\partial t}\right)_{production} = \sigma(eV_d)\; n_o\; \ell_{eff}\; \frac{I_d}{e}$$

If we withdraw the plate from the plasma, the balance equation becomes

$$\left(\frac{\partial N}{\partial t}\right)_{production} = \frac{n_2 V}{\tau}$$

If the production rate and the lifetime of the plasma does not change for the second case,[3] we obtain

$$\frac{n_2 V}{\tau} = \frac{n_1 V}{\tau} + \frac{I_i}{e} \qquad \text{or} \qquad \tau = (n_2 - n_1)V\,\frac{e}{I_i}.$$

i) Using the saturation electron current to obtain the plasma densities, and measuring the extracted ion current I, compute the lifetime.

ii) Estimate the effective path length of the primary electrons, $\ell_{eff}$, and express it in terms of the system diameter.

iii) A more direct method of measuring $\tau$ consists in suddenly terminating the discharge and measuring the decay of the plasma density.

$$\frac{\partial(nV)}{\partial t} = -\,nvA \qquad \text{or} \qquad \tau = \frac{V}{vA}$$

Introduce different areas of loss surface A and check the dependence of $\tau$ on A.

Experimentally the discharge current is repetitively pulsed on and off by a simple transistor circuit as shown in Figure I-6. Plasma characteristics such as density and temperature can be sampled with a boxcar

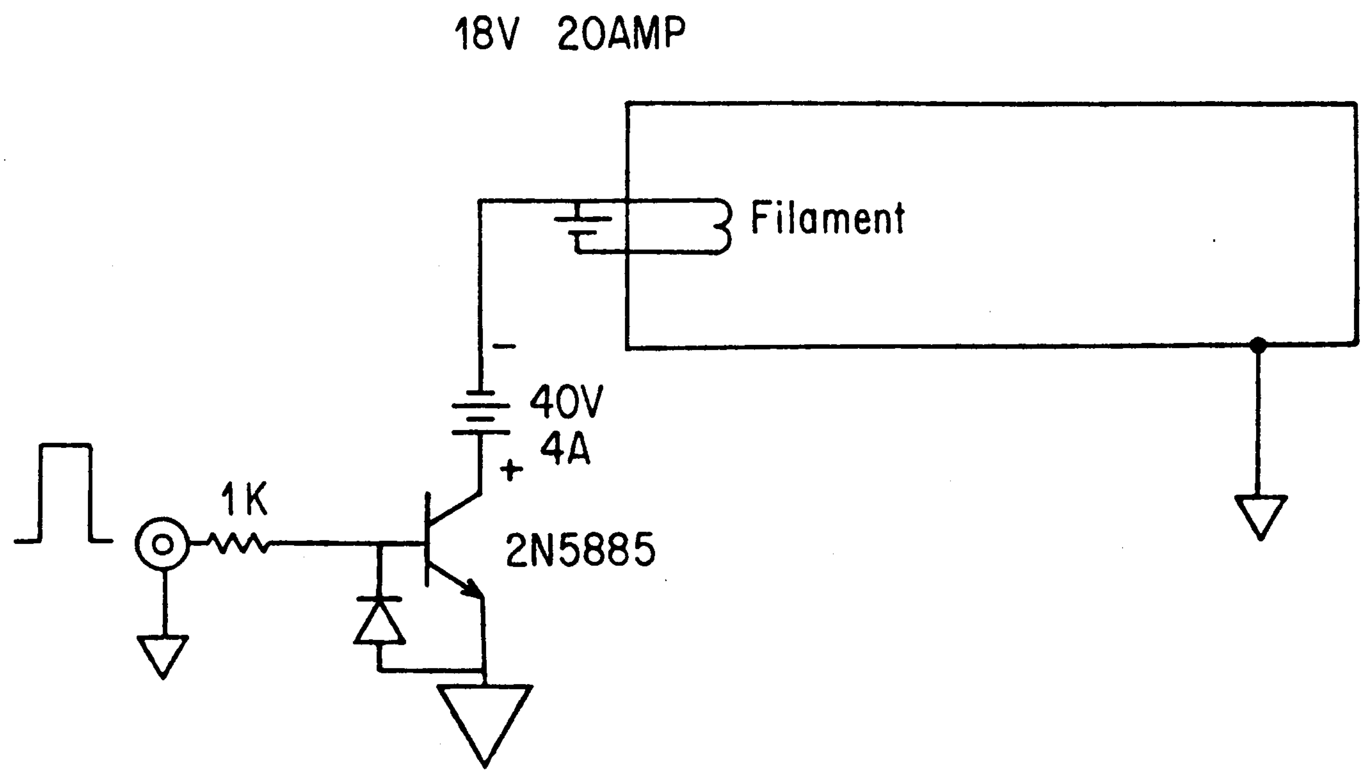


Figure I-6.

Transistor circuit for pulsing discharge current.

integrator or an intensity-modulated scope to be described in Chapter II.

e) Radial density profile: Obtain the radial plasma density profile by monitoring the electron saturation current as a function of radial position. Observe a uniform density in the center region and a steep density gradient in the magnetic field region near the wall. Calculate the density gradient length $L = \left(\frac{1}{n}\frac{dn}{dx}\right)^{-1}$. Can the steep density gradient be explained in terms of plasma production, particle reflection or plasma loss?

f) Quiescence: Monitor the density fluctuations by recording the fluctuations $\Delta I$ about the mean electron saturation current $I_o$. This can be accomplished experimentally by displaying $I_o$ on an oscilloscope and measuring the percentage signal fluctuation. This should be done with a 50 ohm terminating resistor. (Explain)

4) Appendix A: The Vacuum System[4,5]

All vacuum systems used in the plasma physics laboratory employ a water cooled oil vapor diffusion pump backed by a rotary vacuum pump, as sketched in Figure I-7. In the normal mode of operation, valves 1 (high vacuum valve) and 2 (foreline valve) are open and valve 3 (roughing line valve) is closed. In this mode, the diffusion pump is pumping on the system and the rotary (or mechanical pump is pumping on the diffusion pump. The base pressure of the system may be as low as $10^{-6}$ torr (mm Hg) and the foreline pressure should be in the range 1 - 50 microns (1 micron = $10^{-3}$ torr).

The oil diffusion pump cannot pump gases at pressures greater than a few hundred microns. Attempting to operate the pump at pressures greater than this will result in the cracking of the diffusion oil and possibly in the contamination of the system. Never expose a hot diffusion pump to pressures greater than a few hundred microns. If the system is at atmospheric pressure, it must be pumped down to less than 75 microns before the high vacuum valve is opened. This is accomplished by opening valve 3 (with valves 1 and 2 closed) and allowing the mechanical pump to pump the system through the roughing line. When the system pressure is below 75 microns, valve 3 is closed and valves 1 and 2 are opened.

Neutral gas pressure in the system is controlled by valves 4 and 5. Valve 4 functions as on-off valve, while the leak valve controls the gas pressure. The two gases used most frequently in our laboratory are Argon and Helium, and typical operating pressures range from $2 \times 10^{-5}$ torr to $2 \times 10^{-3}$ torr.

Valve 6 is used to bring the system to atmospheric pressure when it is desired to open the plasma chamber.

## Pressure Measurements

The wide range of pressures to be measured necessitates the use of two different types of pressure gauges. The Hastings gauge, a thermocouple type of gauge, can read pressures from about 1 micron to atmosphere. The Hastings gauge serves two purposes in our vacuum systems. When roughing out the system, the Hastings gauge determines when the pressure is low enough to open the high vacuum valve connecting the diffusion pump to the system. When the system is in the normal operating mode, the gauge is used to monitor the foreline pressure.

In the normal operating mode, the system pressure is too low to be read with a Hastings gauge, and an ionization gauge must be used. The ion gauge reads pressure accurately from about $10^{-3}$ to $10^{-8}$ torr. Operation of the gauge at pressures above a few microns for any length of time will severely shorten the tube life. Be sure to turn off the filament of the ion gauge tube whenever the possibility of its being exposed to higher than recommended pressures exists. AC power to the ion gauge, as well as to the Hastings gauge should be left on at all times.

The ion gauge operates by ionizing the gas in the tube and measuring the collected ion current. Therefore, the sensitivity of the gauge depends on the ionization cross section of the gas. The gauge is calibrated for dry air and the correction chart for various gases appears in Table I-2.

## Operating Procedures

When the system is in the normal operating mode only the gas control valves, 4 and 5, need be operated. Valve 4 is opened and the leak valve is adjusted to obtain the desired neutral pressure. Close valve 4 when the experiment is completed.

Except in the event of a major leak, or for maintenance purposes, the diffusion and mechanical pumps are never shut off. If the pumps must be shut off, steps 1 through 4 in the shut down procedure should be followed. To put the system back into operation, follow steps 1 through 5 in the turn on procedure.

The plasma chamber is left under high vacuum except when it is necessary to bring the chamber to atmosphere in order to replace filaments or make other changes. In this case, steps 1 and 2 in the shut down procedure are followed. To resume operation, follow steps 4 through 6 of the turn on procedure.

Turn On Procedure

1. Turn on water cooling for diffusion pump. Shut all valves.
2. Open valve 2 and turn on mechanical pump.
3. When foreline pressure reaches 50 microns or less, turn on diffusion pump. The diffusion pump will take about one half hour to reach operating temperature.
4. When the diffusion pump is hot, close valve 2 and open valve 3 to rough out system.
5. When the system pressure goes below 50 microns, shut valve 3 and open valve 2. Slowly open the high vacuum valve (1), while monitoring the foreline pressure. Do not allow the foreline pressure to go above a few hundred microns. If the foreline pressure does not drop below 1 hundred microns after a few minutes, there is probably a large leak in the system, and the high vacuum valve should be shut.

6. The ionization gauge filament may be turned on after the high vacuum valve has been open a few minutes.

Shut Down Procedure

1. Shut off ionization gauge filament and close high vacuum valve. (Valve 2 should be open and valve 3 closed.)
2. Open valve 6, bringing the plasma chamber to atmospheric pressure.
3. Shut off diffusion pump heater. Allow one half hour for the pump to cool.
4. When the diffusion pump is cool, the mechanical pump and the cooling water may be shut off.

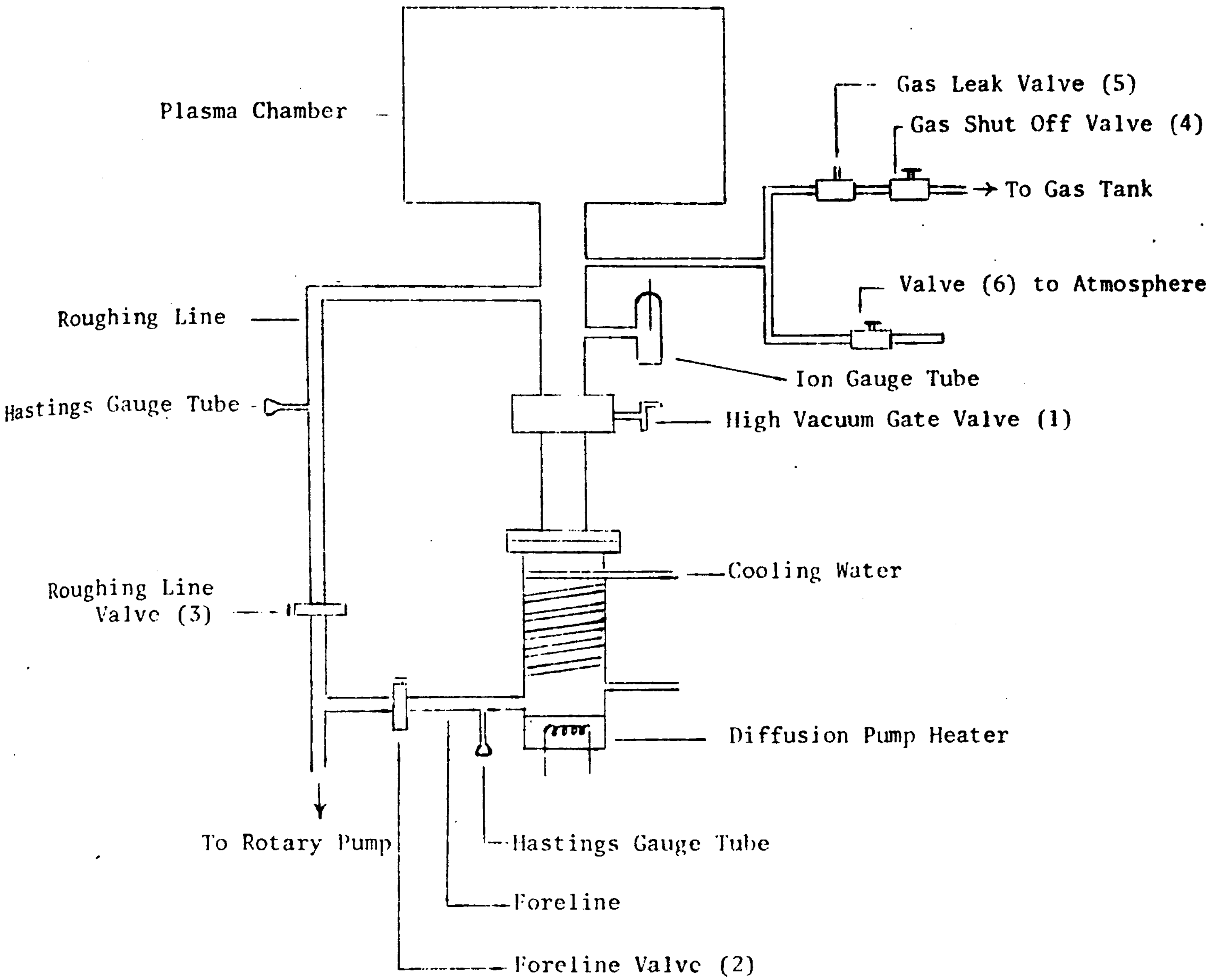


Figure I-7.

Typical Vacuum System

## Chapter II. Basic Plasma Diagnostics

One of the most important and frequently used plasma diagnostic techniques is the Langmuir probe method. This method, which was first introduced by Langmuir[1] about fifty years ago, can be used to determine the values of the ion and electron densities, the electron temperature, and the electron distribution function. This method involves the measurement of electron and ion currents to a small metal electrode or probe as different voltages are applied to the probe. This yields a curve called the probe characteristic of the plasma.

Another important technique, using microwaves, is frequently employed to measure plasma parameters, especially in situations where it is difficult to insert probes into the medium. An interferometer method is used to determine the phase shift of the microwaves transmitted through the plasma and the average electron density is deduced from the amount of phase shift.

By combining the microwave or radio frequency method with the probe technique, we can measure the density to better than 1% accuracy. Electromagnetic waves propagating along a density gradient with frequency $\omega_o$ excite electron plasma waves at the critical density layer $z_o$ for which $\omega_o = \omega_p(z_o)$, where $\omega_p$ is the plasma frequency. Since the propagation of these electron plasma waves is a sensitive function of the density profile, a careful mapping of the electron plasma wave propagation characteristics will reveal the density along its propagation path. This more advanced method is described in Chapter V.

### 1) Langmuir Probe

The fundamental plasma parameters can be determined by placing a small conducting probe into the plasma and observing the current to the probe as a function of the difference between the probe and plasma space potentials. The plasma space potential is just the potential difference of the plasma volume with respect to the vessel wall (anode). It arises from an initial imbalance in electron and ion loss rates and depends in part upon anode surface conditions, and filament emission current.

Referring to the probe characteristic, Figure II-1, we see that in region A when the probe potential, $V_p$, is above the plasma space potential, $V_s$, the collected electron current reaches a saturated level and ions are repelled, while in region B just the opposite occurs. By evaluating the slope of the electron I-V characteristic in region B the electron temperature $T_e$ is obtained, and by measuring the ion or electron saturation current and using the $T_e$ measurement, the density can be computed.

The current collected by a probe is given by summing over all the contributions of the various plasma species:

$$I = A \sum_i n_i q_i \bar{v}_i \tag{1}$$

where A is the total collecting surface area of the probe; $\bar{v}_i$ = the average velocity of species i, and $\bar{v}_i = \frac{1}{n} \int v f_i(\vec{v})\, d\vec{v}$ for unnormalized $f_i(\vec{v})$. It is well known in statistical mechanics that collisions among particles will result in an equilibrium velocity distribution f given by the Maxwellian function:

$$f_\alpha(\vec{v}) = n \left(\frac{2\pi K T_\alpha}{m_\alpha}\right)^{-3/2} \operatorname{Exp}\left(\frac{-\frac{1}{2} m_\alpha |\vec{v}|^2}{K T_\alpha}\right) \tag{2}$$

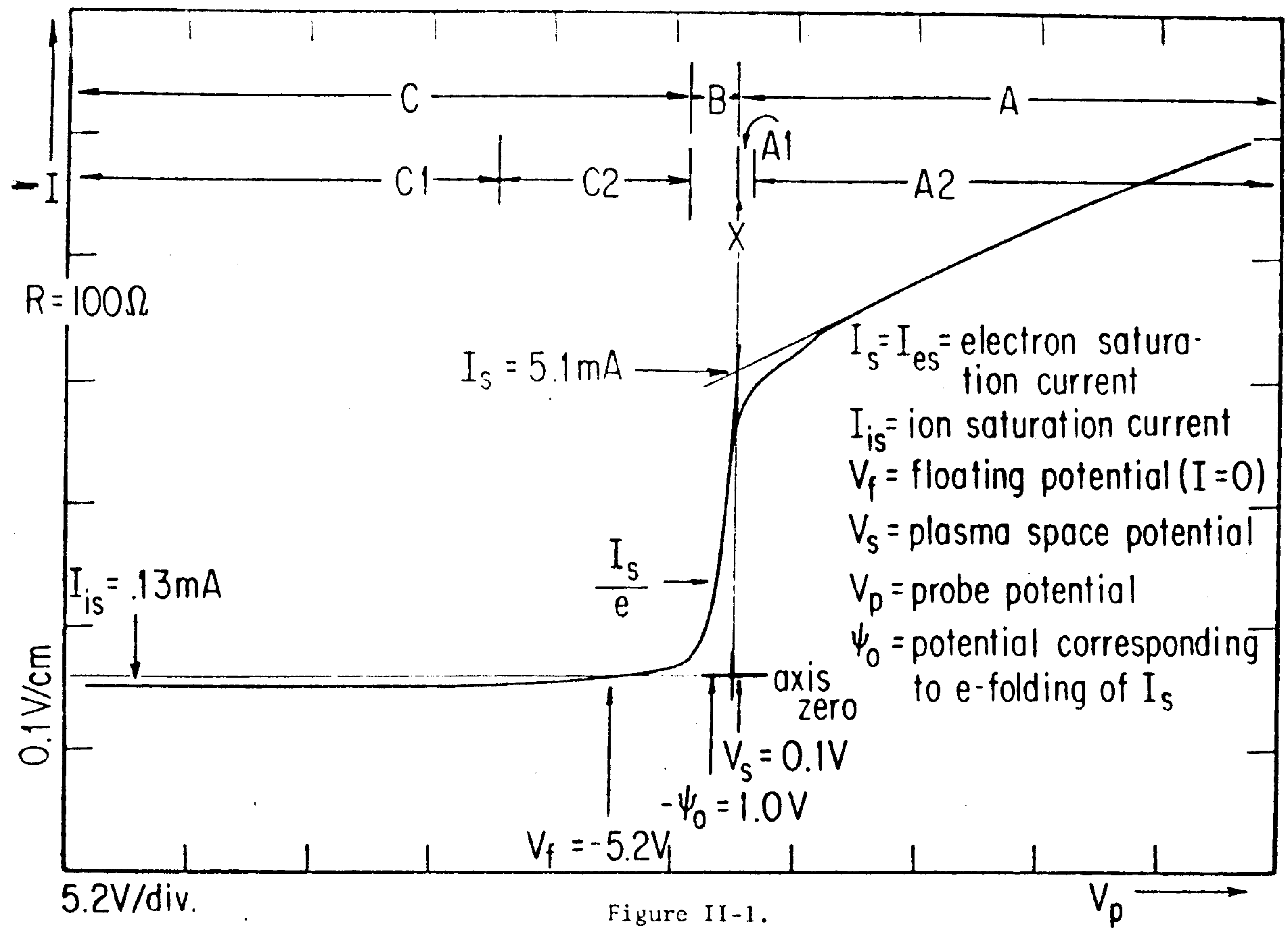


Figure II-1.

Sample Langmuir Probe Characteristic (Radial disc probe placed near center of single plasma): Region C1 - Ion saturation (electrons repelled); Region C2 - Ion saturation plus small primary electron current; Region B - Secondary electrons added to current of primaries and ions; X - Probe at space potential (zero electric probe field); Region A1 - Electron saturation with cooler ions being repelled; Region A2 - Electron saturation, no ion current. Note how $\psi_o$ facilitates identification of secondary electron temperature, $T_e$ (1.0 eV for this data).

This distribution function is used to evaluate the average velocity of each species.

We will first consider a small plane disc probe which is often used in our experiments. When it is placed in the yz plane, a particle will collide with the probe and give rise to a current only if it has some $v_x$ component of velocity. Thus, the current to the probe does not depend on $v_y$ or $v_z$. The current to the probe from each species is a function of $V \equiv V_p - V_s$.

$$I(v) = nqA \int_{-\infty}^{\infty} dv_y \left(\frac{2\pi KT_\alpha}{m_\alpha}\right)^{-\frac{1}{2}} \mathrm{Exp}\left(\frac{-\frac{1}{2}m_\alpha v_y^2}{KT_\alpha}\right) \int_{-\infty}^{\infty} dv_z \left(\frac{2\pi KT_\alpha}{m_\alpha}\right)^{-\frac{1}{2}} \mathrm{Exp}\left(\frac{-\frac{1}{2}m_\alpha v_z^2}{KT_\alpha}\right)$$

$$\cdot \left[ \int_{v_{min}}^{\infty} dv_x v_x \left(\frac{2\pi KT_\alpha}{m_\alpha}\right)^{-\frac{1}{2}} \mathrm{Exp}\left(\frac{-\frac{1}{2} m_\alpha v_x^2}{KT_\alpha}\right)\right]. \qquad (3)$$

The lower limit of integration in the integral over $v_x$ is $v_{min}$ since particles with $v_x$ component of velocity less than $v_{min} = \left(\frac{2qV}{m_\alpha}\right)^{\frac{1}{2}}$ are repelled, Figure II-2.

The integrals over $v_y$ and $v_z$ in (3) give unity so the current of each species is just

$$I(v) = nqA \int_{v_{min}}^{\infty} dv_x v_x \left(\frac{2\pi KT_\alpha}{m_\alpha}\right)^{-\frac{1}{2}} \mathrm{Exp}\left(\frac{-\frac{1}{2}m_\alpha v_x^2}{KT_\alpha}\right). \qquad (4)$$

a) <u>The electron saturation current, $I_{es}$</u>: In this region all electrons with $v_x$ component toward probe are collected. We obtain the electron saturation current

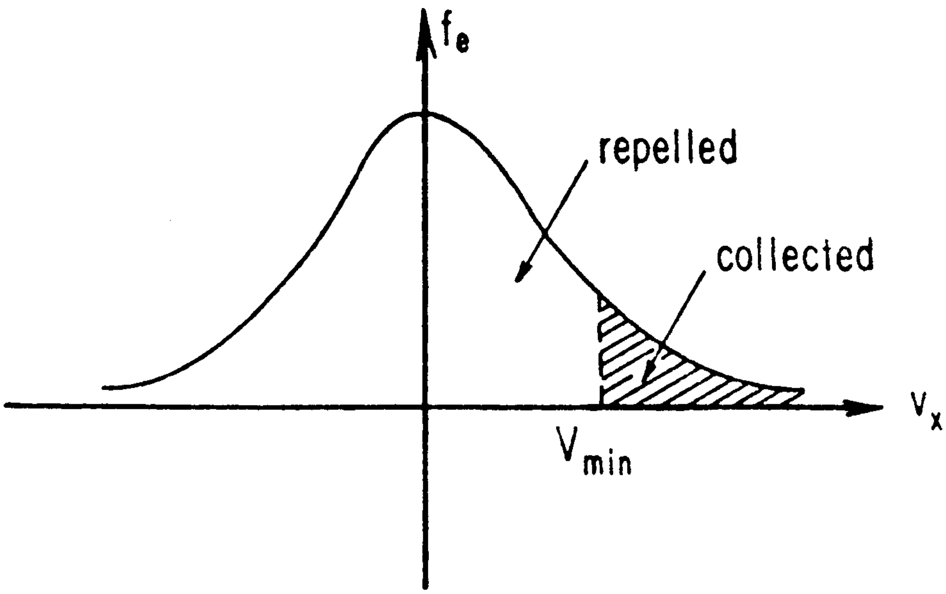


Figure II-2.

Electron Velocity Distribution
All electrons with energy $|eV|$ greater than $\frac{1}{2} m_e v_{min}^2$ are collected.

$$I_{es} = -neA \int_0^\infty dv_x v_x \left(\frac{2\pi KT_e}{m_e}\right)^{-\frac{1}{2}} \text{Exp}\left(\frac{-\frac{1}{2}m_e v_x^2}{KT_e}\right) = -neA\left(\frac{KT_e}{2\pi m_e}\right)^{\frac{1}{2}} \quad (5)$$

Similarly, in region B and C where $V_p < V_s$ and electrons are repelled, the total current is

$$I(v) = I_{is} - neA \int_{v_{min}}^\infty dv_x v_x \left(\frac{2\pi KT_e}{m_e}\right)^{-\frac{1}{2}} \text{Exp}\left(\frac{-\frac{1}{2}m_e v_x^2}{KT_e}\right). \quad (6)$$

Substituting $\frac{1}{2}m_e v_{min}^2 = -eV$, (6) becomes

$$I(v) = I_{is} - neA\left(\frac{KT_e}{2\pi m_e}\right)^{\frac{1}{2}} \text{Exp}\,\frac{eV}{KT_e} \quad (7)$$

since $V < 0$ in region B and C. Equation (7) shows that the electron current increases exponentially until the probe voltage is the same as the plasma space potential ($V = V_p - V_s = 0$).

b) <u>The ion saturation current, $I_{is}$</u>: The ion saturation current is not simply given by an expression similar to (5). In order to repel all the electrons and observe $I_{is}$, $V_p$ must be negative and have a magnitude near $KT_e/e$ as shown in Figure II-3. The sheath criterion[2] requires that ions arriving at the periphery of the probe sheath be accelerated toward the probe with an energy $\sim KT_e$, which is much larger than their thermal energy $KT_i$. The ion saturation current is then approximately given as

$$I_{is} = neA\left(\frac{2KT_e}{m_i}\right)^{\frac{1}{2}}. \quad (8)$$

Even though this flux density is larger than the incident flux density at the periphery of the collecting sheath, the total particle flux is still

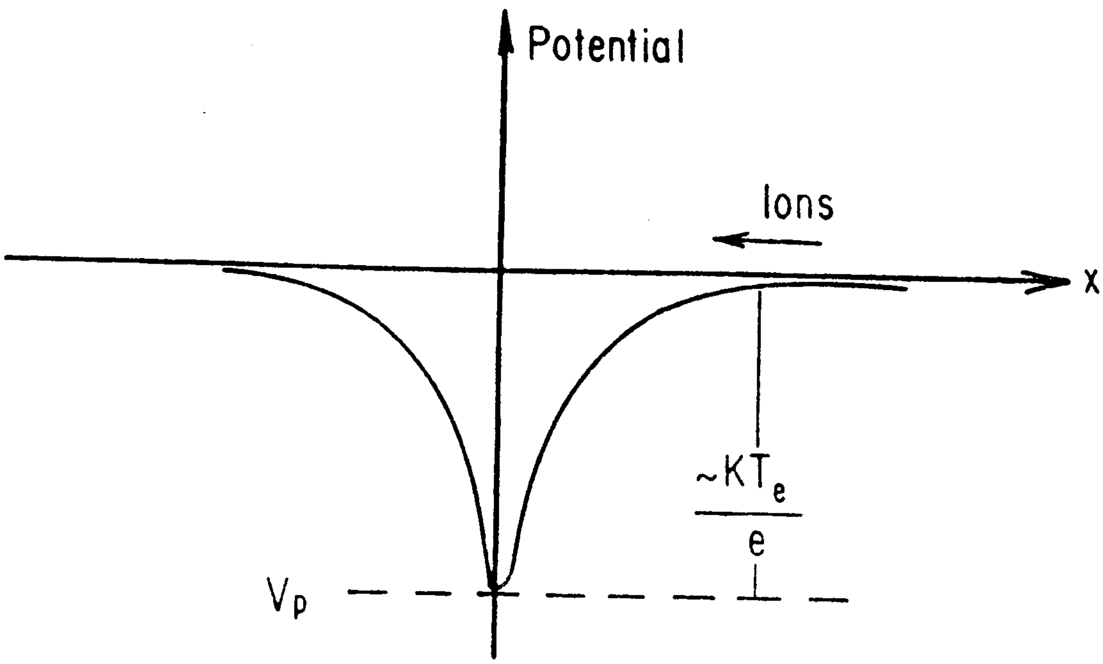


Figure II-3.

Sheath potential as function of distance x from infinite plane probe.

conserved because the area at the probe is smaller than the outer collecting area at the sheath boundary.[2-5]

c) Floating potential, $V_f$: Next we consider the floating potential. When $V = V_f$, the ion and electron currents are equal and the net probe current is zero. Combining equations (7) and (8), and letting I = 0, we get

$$V_f = -\frac{KT_e}{e} \ln \left(\frac{m_i}{4\pi m_e}\right)^{\frac{1}{2}} . \tag{9}$$

d) The electron temperature, $T_e$: Measurement of the electron temperature can be obtained from equation (7). For $I_{is} << I$ we have

$$I(v) \approx -neA \left(\frac{KT_e}{2\pi m_e}\right)^{\frac{1}{2}} \text{Exp}\left(\frac{eV}{KT_e}\right) = I_{es} \text{ Exp}\left(\frac{eV}{KT_e}\right) \tag{10}$$

$$\frac{d \ln |I|}{dV} = \frac{e}{KT_e} . \tag{11}$$

By differentiating the logarithm of the electron current with respect to the probe voltage V for V < 0, the electron temperature is obtained. We note that the slope of $\ln I$ vs. V is a straight line only if the distribution is Maxwellian.

e) Measurement of the electron distribution function, $f_e(v_x)$: The electron current to a plane probe could be written in a more general expression as (again neglecting the ion current)

$$I = nqA \int_{v_{min}}^{\infty} v_x f(v_x) dv_x = \frac{nqA}{m_e} \int_{qV}^{\infty} f(qV)\, d(qV) \tag{12}$$

$$\frac{dI}{d(qV)} \propto f(qV)$$

where $q = -e$, the electron charge. This is a very simple way of obtaining the electron energy distribution function. If we measure $f(v_x)$ as a function of plasma position, we can obtain the <u>phase space distribution</u> $f(v_x, x)$. A further refinement is to observe the distribution at a given time $\tau$ after a certain event using a sampling oscilloscope. This results in the complete description, $f(v, x, \tau)$, of the electrons in a given system.

2) <u>Double Probe</u>[5-6]

A double probe consists of two electrodes of equal surface area, separated by a small distance and immersed in the plasma, Figure II-4. One probe draws current $I_1$ while the other is drawing current $I_2$. To find the electron temperature of the plasma, we consider quantitatively the current to the probe for various potential differences between the probes, Figure II-5. Since the probes are floating at $V_f$ of the plasma, i.e., the double probe circuit has no plasma ground (anode) connection, the total current in the probe circuit must be zero. From (7) and (5), the current collected by probe #1 is

$$I_1 = I_{1\,is} - I_{1\,es} \;\mathrm{Exp}\left(\frac{e(V_1 + V_f - V_s)}{KT_e}\right) \tag{13}$$

Using the definition of the floating potential with (7),

$$I_{es} \;\mathrm{Exp}\left(\frac{e(V_f - V_s)}{KT_e}\right) = I_{is}\ , \tag{14}$$

hence (13) becomes

$$I_1 = I_{1\,is}\left[1 - \mathrm{Exp}\left(\frac{eV_1}{KT_e}\right)\right]. \tag{15}$$

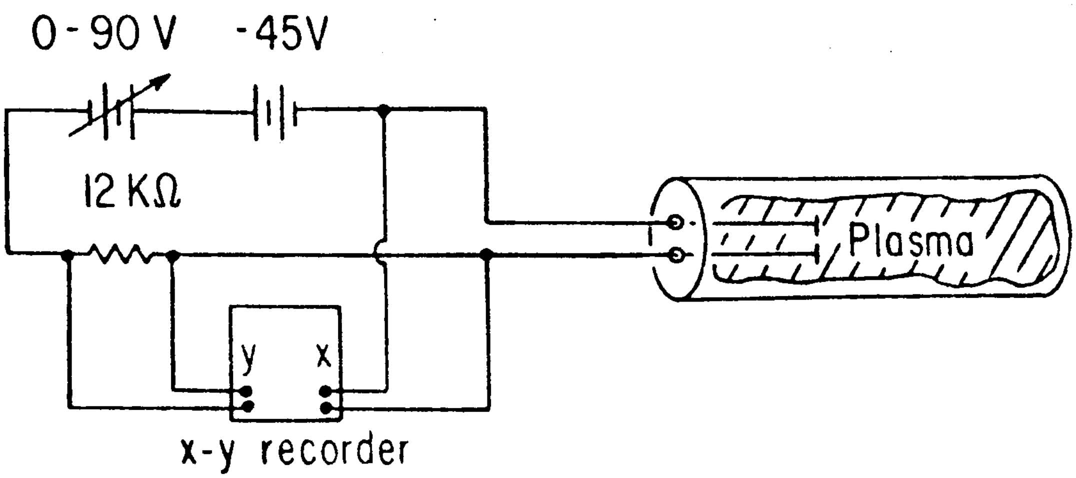


Figure II-4.

Typical Double Probe Manual Sweep Circuit. Note that there is no connection made to plasma ground in this diagnostic; it is independent of plasma potential.

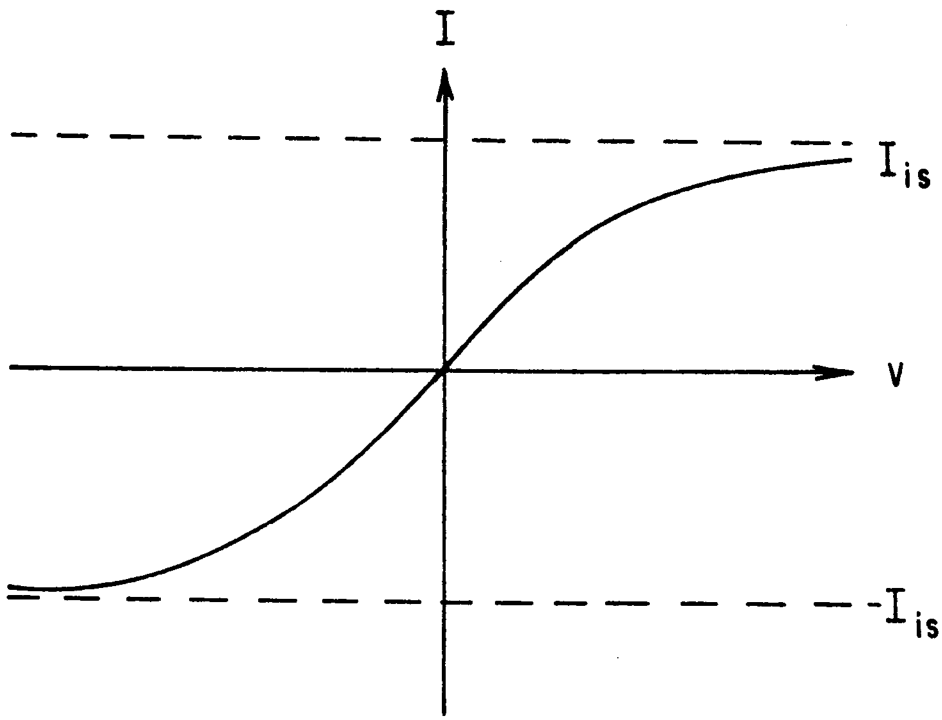


Figure II-5.

Current vs. voltage characteristic of a double probe.

In the same manner we get

$$I_2 = I_{2\,is}\,[1 - \mathrm{Exp}\left(\frac{eV_2}{KT_e}\right)]. \tag{16}$$

If the probe areas are equal, then (8) implies

$$I_{1\,is} = I_{2\,is} = I_{is}. \tag{17}$$

Zero net probe circuit current motivates the definition

$$I \equiv I_1 = - I_2.$$

Combining this with equations (15), (16) and (17) yields

$$\frac{I - I_{is}}{-I - I_{is}} = \mathrm{Exp}\left(\frac{e\psi}{KT_e}\right) \tag{18}$$

where the double probe potential is defined by $\psi \equiv V_1 - V_2$. Solving equation (18) for I

$$I = -I_{is}\tanh\left(\frac{e\psi}{2KT_e}\right) \tag{19}$$

Differentiating equation (19) with respect to $\psi$ at $\psi = 0$

$$\left.\frac{dI}{d\psi}\right|_{\psi = 0} = -I_{is}\left.\mathrm{sech}^2\frac{e\psi}{2KT_e}\right|_{\psi = 0}\left(\frac{e}{2KT_e}\right) \tag{20}$$

i.e., electron temperature is related to the slope of the double probe characteristic by

$$\left.\frac{dI}{d\psi}\right|_{\psi = 0} = -I_{is}\left(\frac{e}{2KT_e}\right) \tag{21}$$

The double probe can collect a maximum current equal to the ion saturation current and does not disturb the plasma as much as the single probe with its anode connection. However, the small amount of detected current (microampere range) does warrant a much more sensitive detection circuit, as in Figure II-4.

The student is required to compare the electron temperatures and plasma densities obtained with the single and the double probes.

3) Microwave Interferometer[9, 10]

The basic idea behind this diagnostic scheme is as follows. The plasma acts like a dielectric medium to electro magnetic radiation, and a wave propagating through the plasma will suffer a change in phase

$$\Delta\phi = \int_0^L (k_{vacuum} - k_{plasma})\, dx \tag{22}$$

where L is the path length of the plasma, $k_{vacuum} = \frac{\omega}{c}$ is the free space wave number of the electromagnetic waves, and $k_{plasma}$ is the wave number of the wave propagating in the plasma, which is given by the dispersion relation

$$k_{plasma} = \frac{(\omega^2 - \omega_{pe}^2)^{\frac{1}{2}}}{c} \tag{23}$$

Here $\omega$ is the wave frequency, $\omega_{pe} = \left(\frac{4\pi ne^2}{m}\right)^{\frac{1}{2}}$, the electron plasma frequency and c is the speed of light. If the plasma density is uniform over the distance L, we obtain from equation (23) for the phase shift

$$\Delta\phi = \frac{\omega}{c}\left[1 - \left(1 - \frac{\omega_{pe}^2}{\omega^2}\right)^{\frac{1}{2}}\right] L. \tag{24}$$

a) <u>Density measurement by phase shift</u>: When $\omega_{pe} << \omega$ (note this restriction) we obtain a relation between the phase shift and plasma density

$$\Delta\phi = \frac{\omega}{c}\left(\frac{1}{2}\frac{\omega_{pe}^{2}}{\omega^{2}}\right)L. \tag{25}$$

Defining the critical density by $\frac{4\pi n_c e^2}{m_e} \equiv \omega^2$ we can express equation (25) alternatively by

$$\frac{n}{n_c} = \frac{2\Delta\phi}{k_{vac}L}, \quad \text{where } k_{vac} \equiv \frac{w}{c} \tag{26}$$

Since all laboratory plasmas have a certain degree of inhomogeneity, i.e., some density gradient, the phase shift $\Delta\phi$ is an integrated quantity as represented by equation (23). However, the density profile can be obtained by relative density measurement using movable probes. If we write $n(x) = n_o f(x)$, where $f(x)$ contains the spatial variation in the plasma density, a relation similar to equation (26) can be achieved using

$$n_o = \frac{2n_c\Delta\phi}{k_{vac}\int_o^L f(x)dx} \tag{27}$$

Thus with the help of the radial probe measurement on the relative density profile, the microwave interferometer technique could be used to obtain the absolute density at any radial position.

b) <u>Observation of cut-off</u>: For $\omega \approx \omega_{pe}$, the relation given by equation (26) or (27) is no longer valid (why?). One must use equation (23) or (24) directly and the relation between $\Delta\phi$ and n becomes quite complicated. However, when $\omega \leq \omega_{pe}$, the wave number becomes purely imaginary and no propagation is possible. By observing the cut-off, we can calculate the maximum density in the plasma, $n_{max} = n_c$, where $n_c$ is the critical density defined above. The student is required to compare this microwave method with the Langmuir probe result.

4) Experimental Procedure

a) Follow the procedure as described in Chapter I to obtain a D.C. discharge. Clean up probes and set up a sweeper circuit as described in Appendix A. Observe a Langmuir characteristic curve by using the oscilloscope. For recording, the single sweep mode must be used with sweep rate of 1 to 2 seconds per cm, such that the mechanical movement of the recorder pin can follow the changes of the signal. The manual sweeping circuit of Figure II-7a is a possible substitute for oscilloscope and automatic sweeper when recording the Langmuir curve graphically.

b) Details of the probe characteristic: Take several single probe traces using the probe sweeper circuit and the x-y recorder. Replot each trace on semi-log paper and subtract out the ion saturation current to obtain the current contributed by the secondary electrons. At low neutral pressures the primary electron current will appear as a long, high temperature (gently sloping) tail with negative current in the ion saturation region of probe bias. In this case, subtract the primary electron current (as well as the ion saturation current) from the total probe current to obtain actual secondary electron current. (Primary electron current collected for a given probe bias can be estimated by extrapolating the straight-line primary tail.) Obtain the electron temperature from the slope of the curve and the density from both the ion and electron saturation currents. Experimentally determine how the ratio $I_{es}/I_{is}$ depends on the mass ratio.

You will find that the primary electron current usually overshadows the ion current. However, the ratio of primary electron to ion current can be reduced significantly and the ion saturation current can be observed by simply raising the neutral pressure to about $10^{-3}$ torr (explain why).

c) Double probe: Set up the double probe manual sweeper circuit with the x-y recorder and obtain a double probe trace. Compute the density and electron temperature and compare the result with n and $T_e$ obtained from a single probe characteristic at the same time in the same region of the plasma.

d) Microwave interferometer: The X-band microwave interferometer set-up is shown in Figure 11-6. Microwave signal generated by the oscillator is split into two paths, one propagating through the plasma, $V_1 \cos(\omega t + \phi_1)$, the other through a variable phase shifter to provide a reference signal, $V_2 \cos(\omega t + \phi_2)$. The signal propagating through the plasma is received by a pickup horn on the other side of the vacuum system, and then added to the reference signal by the magic tee: $V_{sum} = V_1 \cos(\omega t + \phi_1) + V_2 \cos(\omega t + \phi_2)$. This signal is then fed into a crystal detector, which produces a current signal $I \propto V^2_{sum}$. By taking a time average of the current I from the crystal,

$$\langle I\rangle \propto \langle V_{sum}{}^2\rangle = \frac{1}{2}V_1{}^2 + \frac{1}{2}V_2{}^2 + V_1V_2 \cos(\phi_1 - \phi_2). \quad (28)$$

For a given plasma density, $\phi_1$ is fixed. Vary $V_2$ with the variable attenuator and $\phi_2$ with the phase shifter to obtain a null ($\phi_1 - \phi_2 = \pi$). Be careful not to overattenuate the reference signal $V_2$ as this will result in a phase independent signal [$V_2 = 0$ in (28)].

The crystal diode output signal is so small that a high gain amplifier must be used. Furthermore, the microwave signal should be gated on and off

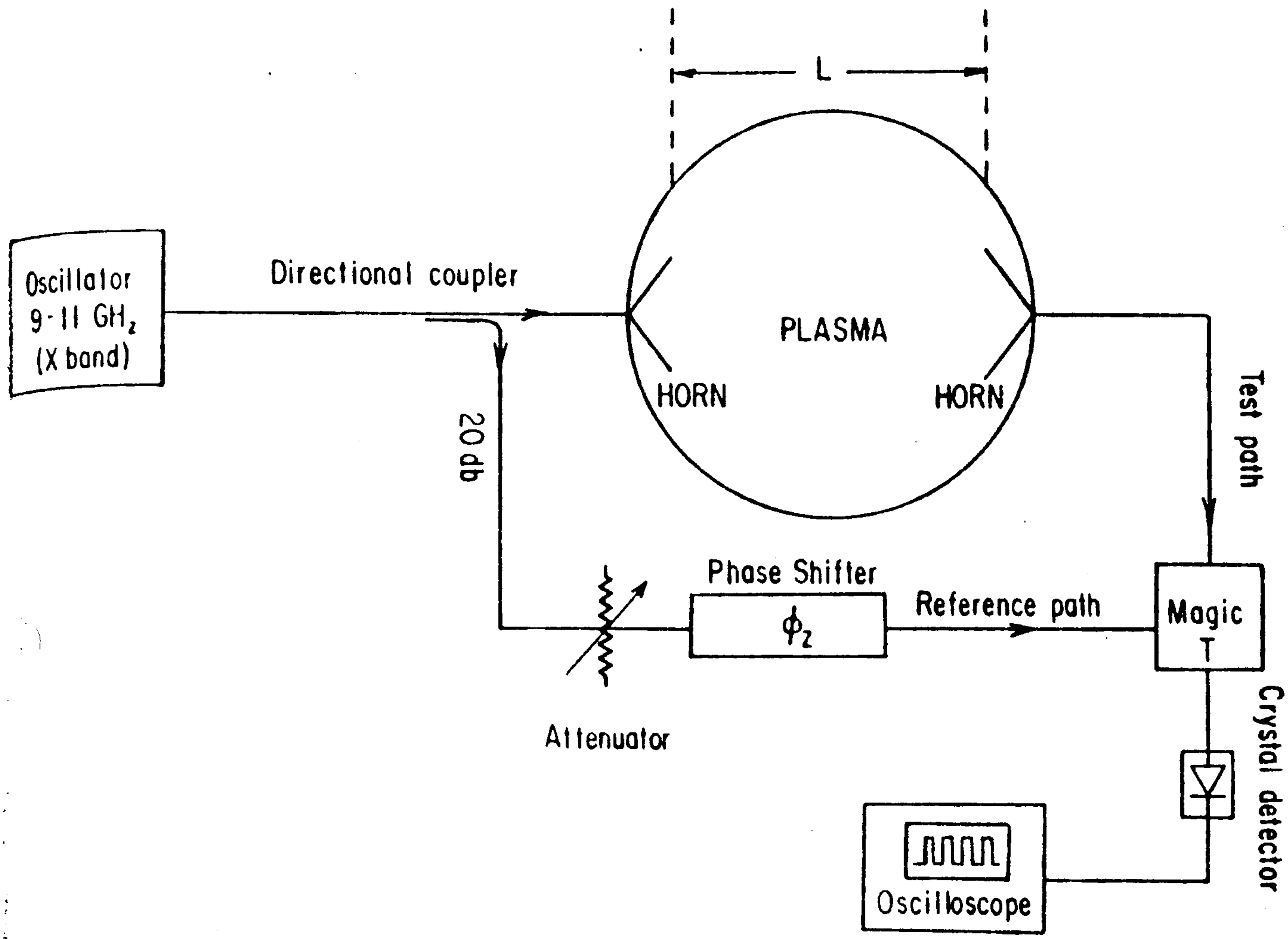


Figure II-6.

Interferometer Setup

(i.e., square wave modulated output) to avoid confusion over D.C. shifting of the output signal in the high gain amplifier.

Turn off the plasma (by turning off the discharge), find the null again and record $\Delta\phi$. In finding the null, large errors can develop. To minimize these, plot $\langle V_{sum}^2 \rangle$ versus $\phi_z$ for the case where the plasma is present and the case where it is turned off to obtain two cosine curves offset by phase $\Delta\phi$. Although this procedure is tedious, it is recommended for improved accuracy.

Calculate the plasma density using equation (26) and compare the results with those obtained from the probe measurements. If the density is non-uniform, try to correct the result by measuring relative density profile using a movable Langmuir probe. Difficulties arise whenever the dimensions of the plasma container are comparable to the wavelength of the microwaves. In this case, the waveguide horn is not large enough to sharply define the microwave beam and unwanted cavity modes are excited in the vacuum chamber as a result. These modes have multiple paths through the plasma and can drastically alter the measurement of $\Delta\phi$. Hence, steel wool has been placed near both the sending and receiving horns to attenuate these undesirable multiple path signals.

e) Density Measurement via Plasma Resonance: The most accurate local density measurement in an inhomogeneous plasma is achieved by exciting the local plasma resonance $\omega_p(x)$. An oscillating electric field of frequency $\omega_o$ is externally excited in the plasma by a capacitor plate oriented to give an electric field along the density gradient as shown in Figure II-7. Wherever the external frequency matches the local plasma frequency $\omega_o = \omega_p(x_o)$, the amplitude of the external electric field is found to be enhanced by an order of magnitude or more. This resonance is best detected by noting the deflection of an electron beam traversing the resonant location (Figure II-7) in a direction perpendicular to the density gradient. (A detailed description of this electron beam diagnostic is to be presented in Chapter V.) Since the extermal oscillating field frequency $\omega_0$ can be precisely measured, the plasma density can be determined to better than 1%. A Langmuir probe can be calibrated using this technique.

QUESTIONS

1. Why does the ion saturation current depend on $\kappa T_e$?
2. If there is an excess of primary electrons in the plasma, what kind of effect can one see by using (1) single probe, (2) double probe and (3) microwave interferometer? Can you measure the density of the primary electrons?
3. For a plasma consisting of positive and negative ions of equal mass, draw the probe characteristics, carefully labeling the quantities $I_{s+}$, $I_{s-}$, $V_f$ and $V_s$. How do you deduce $T_+$ and $T_-$?
4. What processes determine potential difference between the plasma and the anode?
5. When a fine conducting grid (called "plasma demon") is biased to some positive potential, it was found that the electron temperature increases by a factor up to 2 - 3. Can you explain this effect?

sheet velocity of $7 \times 10^6$ cm/sec. The apparent current sheet thickness is then 5 mm, and we conclude that the conduction hole around the probe can be no larger than this. (The probe itself was 3 mm in diameter.) Portions of the field distribution having more gentle structure than this may then be assumed to be accurately rendered.

## References


1. T. Ohkawa, H. K. Forsen, A. A. Schupp, Jr., and D. W. Kerst. *Phys. Fluids* **6**, 846 (1963).
2. I. N. Golovin, D P. Ivanov, V. D. Kirillov, D. P. Petrov, K. A. Razumova, and N. A. Yavlinsky, *Proc. 2nd Intern. Conf. Peaceful Uses At. Energy, Geneva, 1958* Vol. 32, p. 72 (I. D. S. Columbia Univ. Press, New York, 1959).
3. J. C. Keck, *Phys. Fluids* **5**, 630 (1962).
4. L. O. Heflinger and S. L. Leonard, *Phys. Fluids* **4**, 406 (1961).
5. R. H. Lovberg, *Proc. 6th Intern. Conf. Ionization Phenomena in Gases, Paris, 1963* Paper IX, 6 (North-Holland, Amsterdam, 1964), in press; also *Gen. Dynamics Corp. (San Diego) Rept.* No. GA-4363 (1963).
6. L. C. Burkhardt and R. H. Lovberg, *Phys. Fluids* **5**, 341 (1962).
7. J. L. Tuck, *Proc. 2nd Intern. Conf. Peaceful Uses At. Energy, Geneva, 1958* Vol. 32, p. 9 (I. D. S. Columbia Univ. Press, New York, 1959).
8. L. C. Burkhardt and R. H. Lovberg, *Proc. 2nd Intern. Conf. Peaceful Uses At. Energy, Geneva, 1958* Vol. 32, p. 31 (I. D. S. Columbia Univ. Press, New York, 1959).
9. D. A. Baker, G. A. Sawyer, and T. F. Stratton, *Proc. 2nd Intern. Conf. Peaceful Uses At. Energy, Geneva, 1958* Vol. 32, p. 34 (I. D. S. Columbia Univ. Press, New York, 1959).
10. R. F. Post, *Ann. Rev. Nucl. Sci.* **9**, 367 (1958).
11. D. Bohm, with E. H. S. Burhop and H. S. W. Massey, *in* "The Characteristics of Electrical Discharges in Magnetic Fields" (A. Guthrie and R. K. Wakerling, eds.), p. 13. McGraw-Hill, New York, 1949.
12. K. Yamamoto and T. Okuda, *J. Phys. Soc. Japan* **11**, 57 (1956).
13. S. Glasstone and R. H. Lovberg, "Controlled Thermonuclear Reactions," p. 470. Van Nostrand, Princeton, New Jersey, 1960.
14. L. Spitzer, Jr., "The Physics of Fully Ionized Gases," p. 87. Wiley (Interscience), New York, 1956.
15. D. E. T. F. Ashby, *J. Nucl. Energy, Pt. C* **5**, 83 (1962).
16. F. Jahoda and G. Sawyer, *Phys. Fluids* **6**, 1195 (1963).
17. J. H. Malmberg, *Rev. Sci. Instr.* **35**, 11, 1622 (1964).
18. G. Ecker, W. Kröll, and O. Zöller, *Ann. Physik* [7] **10**, 222 (1962).
19. D. F. Brower, R. E. Dunaway, J. H. Malmberg, C. L. Oxley, M. Stearns, D. W. Kerst, F. R. Scott, S. P. Cunningham, and R. G. Tuckfield, Jr., *Proc. 2nd Intern. Conf. Peaceful Uses At. Energy, Geneva, 1958* Vol. 32, p. 110. I. D. S. Columbia Univ. Press, New York, 1959).
20. A. M. Andrianov *et al.*, *in* "Plasma Physics and the Problems of Controlled Thermonuclear Reactions" (Acad. Sci. U.S.S.R., M. A. Leontovich and J. Turkevich, eds.), Vol. II, p. 274. Macmillan (Pergamon), New York, 1959.


EXP #5.

From Plasma Diagnostic Techniques Ed. Huddlestone and Leonard (Acad. Press, 1965)

*Chapter 4*

# Electric Probes

***Francis F. Chen***



## 1 Introduction

One of the fundamental techniques—the first one, in fact—for measuring the properties of plasmas is the use of electrostatic probes. This technique was developed by Langmuir as early as 1924 and consequently is sometimes called the method of Langmuir probes. Basically, an electrostatic probe is merely a small metallic electrode, usually a wire, inserted into a plasma. The probe is attached to a power supply capable of biasing it at various voltages positive and negative relative to the plasma, and the current collected by the probe then provides information about the conditions in the plasma.

It is a fortunate property of plasmas that under a wide range of conditions the disturbance caused by the presence of the probe is localized, and the probe can act truly as a probe in the sense that its very presence has no effect on the quantities it is measuring. We shall find, however, that under certain circumstances, particularly in the presence of a strong magnetic field, the disturbance is *not* localized, and the probe current then depends not only on the plasma parameters (density and electron and ion temperatures), but also on the way in which the plasma is created and maintained. In such a case the method becomes obviously less useful.

In spite of the difficulties which arise when probes are used in present-day plasmas, the method is an important one because it has one advantage over all other diagnostic techniques: it can make local measurements. Almost all other techniques, such as spectroscopy or microwave propagation, give information averaged over a large volume of plasma.

Experimentally, electrostatic probes are extremely simple devices, consisting merely of an insulated wire, used with a dc power supply, and an ammeter or an oscilloscope. Nature, however, makes us pay a penalty for this simplicity: the theory of probes is extremely complicated. The difficulty stems from the fact that probes are boundaries to a plasma, and near the boundary the equations governing the motion of the plasma change their character. In particular, the condition of quasi-neutrality, which obtains in the body of the plasma, is not valid near a boundary; and a layer, called a "sheath," can form, in which ion and electron densities can differ and hence large electric fields can be sustained. A fundamental result of the original work of Langmuir and H. M. Mott-Smith, Jr. (see *1*, pp. 23–132) was that in many cases the sheath could be considered a thin layer near the probe surface and that the quasi-neutral equation could be used up to a "sheath edge," which in practice had a well-defined position. In recent years considerable progress has been made in the application of boundary-layer techniques to this problem, so that the artifice of a sheath edge has been removed and the continuous transition from boundary to plasma can be described, at least in the collisionless case. The sheath then appears as a natural consequence of the nature of the mathematical equations, and the accuracy of the approximations which Langmuir made with great insight in the early days of plasma physics has been borne out in a large number of physically interesting cases.

It will be our purpose to summarize the available theoretical results, giving a sketch wherever possible of the way in which they were obtained, and to supplement this with practical information on experimental techniques. In Sec. 2 we begin with a short introduction to the physical notion of sheath. In Sec. 3 we shall present the well-documented theory of probes in a collisionless plasma. Although the theory of probes in the presence of collisions and magnetic fields is still in a primitive state, we shall treat this in some detail in Secs. 4 and 5 because of the current interest in magnetically confined plasmas. In the final sections we shall describe specialized techniques and practical considerations in the use of electrostatic probes. Quantities will be in cgs–es units.

The literature on probes is so extensive that we have not attempted to include here a complete survey of it. However, we have tried to include references to the most recent papers, from which references to earlier works can be obtained.

In order to get an over-all view of the situation, let use look at a physical plot of probe current versus probe voltage, as shown in Fig. 1. Here negative, or electron, current to the probe is plotted against $V_p$, the probe voltage with respect to an arbitrary reference point. This plot may be obtained continuously in a steady-state discharge, or point by point in a pulsed discharge, the probe bias being changed from pulse to

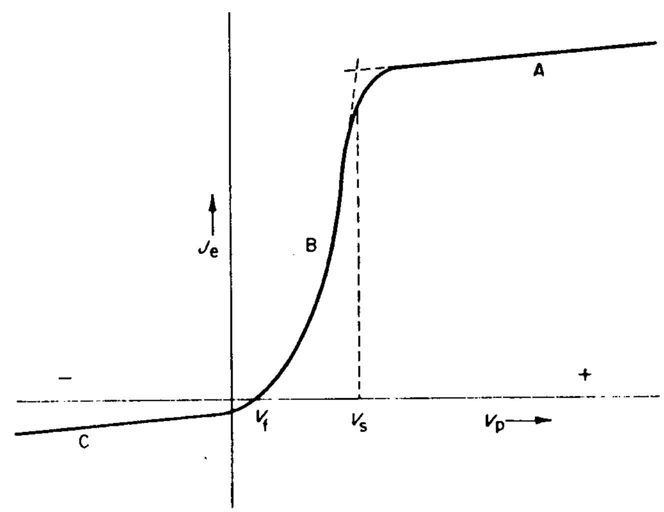


Fig. 1. Schematic of a typical probe current-voltage characteristic.

pulse; or the ͏ire curve may be obtained in a few microseconds in a pulsed discharge by the use of a fast-sweeping voltage source.

The qualitative behavior of this curve can be explained as follows. At the point $V_s$, the probe is at the same potential as the plasma (this is commonly called the space potential). There are no electric fields at this point, and the charged particles migrate to the probe because of their thermal velocities. Since electrons move much faster than ions because of their small mass, what is collected by the probe is predominantly electron current. If the probe voltage is made positive relative to the plasma, electrons are accelerated toward the probe. Moreover, the ions are repelled, and what little ion current was present at $V_s$ vanishes. Near the probe surface there is therefore an excess of negative charge, which builds up until the total charge is equal to the positive charge on the probe. This layer of charge, the sheath, is usually very thin, and outside of it there is very little electric field, so that the plasma is undisturbed. The electron current is that which enters the sheath through random thermal motions; and since the area of the sheath is relatively constant as the probe voltage is increased, we have the fairly flat portion $A$ of the probe characteristic. This is called the region of saturation electron current.

If now the probe potential is made negative relative to $V_s$, we begin to repel electrons and accelerate ions. The electron current falls as $V_p$ decreases in region $B$, which we shall call the transition region or retarding-field region of the characteristic. If the electron distribution were Maxwellian, the shape of the curve here, after the contribution of ions is subtracted, would be exponential. Finally, at the point $V_f$, called the floating potential, the probe is sufficiently negative to repel all electrons except a flux equal to the flux of ions, and therefore draws no net current. An insulated electrode inserted into a plasma would assume this potential.

At large negative values of $V_p$ almost all the electrons are repelled, and we have an ion sheath and saturation ion current (region $C$). This is similar to region $A$; but there are two points of asymmetry between saturation ion and saturation electron collection aside from the obvious one of the mass difference, which causes the disparity in the absolute magnitude of the currents. The first point is that the ion and electron temperatures are usually unequal, and it turns out that sheath formation is considerably different when the colder species is collected than when the hotter species is collected. The second point is that when there is a magnetic field, the motion of the electrons is much more affected by the field than the motion of the ions. These two points, which were neglected in the original theory of Langmuir, are responsible for making impossible the simple and straightforward application of probes as originally proposed by Langmuir.

If it is possible to place a probe in a plasma in such a way that the plasma is not greatly disturbed by the probe, then one can hope to obtain from the probe characteristic information regarding the local plasma density $n$, electron temperature $kT_e$, and space potential $V_s$. The shape of part $B$ of the characteristic obviously is related to the distribution of electron energies and hence gives $kT_e$ when the distribution is Maxwellian. The magnitude of the saturation electron current is a measure of $n(kT_e)^{1/2}$, from which $n$ can be obtained. The magnitude of the ion saturation current depends on $n$ and $kT_e$, but only slightly on $kT_i$, at least in the usual case where $kT_i \ll kT_e$; hence ion temperature is not easily measured with probes. Finally, the space potential can be measured by locating the junction between parts $A$ and $B$ of the curve or by measuring $V_f$ and calculating $V_s$. In the presence of collisions or magnetic fields, the probe currents depend also on the transport coefficients of the plasma. In many instances, such as in a magnetic field, the absolute magnitude of $n$ cannot be calculated with certainty; however, probes are still useful for finding the relative density in different parts of the plasma. In unstable plasmas probes are useful for measuring fluctuations in $n$ or $V_s$, which are simply related to fluctuations in probe current or floating potential.

## 2 Sheath Formation

### 2.1 The Debye Shielding Length

Let us consider the effect of introducing a potential $V_0$ at some point $x = 0$ in a plasma of dimensions $R$ and undisturbed density $n_0$. The potential is given by Poisson's equation, which, for simplicity, we write in one dimension:

$$\frac{d^2V}{dx^2} = -4\pi e(n_i - n_e). \tag{1}$$

If we normalize $V$, $n_i$, $n_e$, and $x$ as follows:

$$\eta = -\frac{eV}{kT_e}, \quad \nu_i = \frac{n_i}{n_0}, \quad \nu_e = \frac{n_e}{n_0}, \quad \xi = \frac{x}{R}, \tag{2}$$

the equation becomes

$$\frac{h^2}{R^2}\frac{d^2\eta}{d\xi^2} = \nu_i(\eta) - \nu_e(\eta), \tag{3}$$

where

$$h \equiv (kT_e/4\pi n_0 e^2)^{1/2}. \tag{4}$$

Since the quantity $h/R$ is small in a plasma (by definition), Eq. (3) has the appearance of a boundary-layer equation; that is, the highest derivative in the equation is multiplied by a very small number. This means that the equation without the derivative, $\nu_e = \nu_i$, which is called the "quasi-neutral equation" or the "plasma equation," is valid over scale lengths of the order of $R$ and that $\eta$ changes considerably only within a small length of the order of $h$ next to the boundary in order to satisfy the boundary condition at $\xi = 0$.

For example, let the ions be infinitely massive, so that $n_i$ is constant, and let the electrons be in thermal equilibrium:

$$n_e = n_0 e^{-\eta}. \tag{5}$$

Poisson's equation then takes the form

$$\frac{d^2\eta}{d(x/h)^2} = 1 - e^{-\eta} \approx \eta. \tag{6}$$

Thus for small $\eta$ the potential decays like

$$V = V_0 e^{-(x/h)}, \tag{7}$$

and the externally imposed potential is shielded within a distance of the order of $h$. The length $h$ is called the Debye shielding length.

## 2.2 THE CHILD-LANGMUIR LAW

Let us now examine another idealized situation, that of two infinite plane-parallel plates, one which emits particles and is at zero potential, and the other which is perfectly absorbing and is at a potential $V_B$. This is shown in Fig. 2.

Consider first the case of emission at plane $A$ of only one species of particle, with charge $-e$ and mass $m$, emitted at zero velocity. The particle velocity at a position where the potential is $V$ is then

$$v = (2eV/m)^{1/2}. \tag{8}$$

If the emitted particle current density is $j$, the particle density at $x$ will be

$$n(x) = j[2eV(x)/m]^{-1/2}. \tag{9}$$



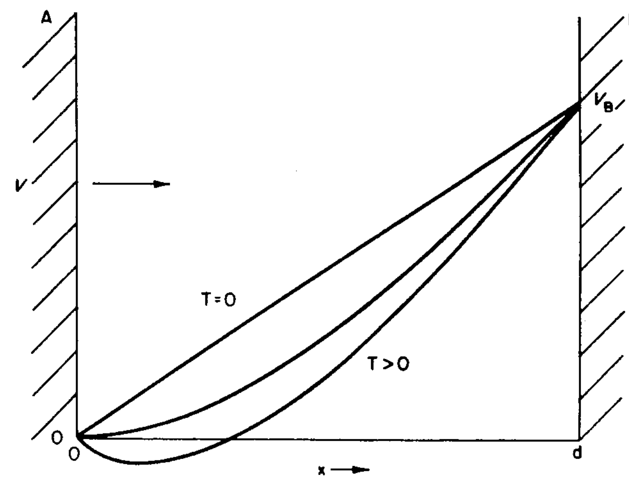


FIG. 2. Schematic of the potential distribution between two planes, one of which is emitting electrons.

Poisson's equation becomes

$$d^2V/dx^2 = 4\pi ej(2eV/m)^{-1/2}.$$

Multiplying by $dV/dx$ and integrating from $x = 0$, we have

$$\begin{aligned} \frac{1}{2}\left(\frac{dV}{dx}\right)^2 &= 4\pi ej \int_0^V \left(\frac{2eV}{m}\right)^{-1/2} dV \\ &= 4\pi j(2me)^{1/2} V^{1/2} + \left(\frac{dV}{dx}\right)_0. \end{aligned} \tag{10}$$

By space-charge-limited flow, we mean that $(dV/dx)_0$ vanishes. We then have

$$V^{-1/4}\, dV = (8\pi j)^{1/2}(2me)^{1/4}\, dx. \tag{11}$$

Integrating from $x = 0$ to $x = d$, we have

$$\tfrac{4}{3} V_B^{3/4} = (8\pi j)^{1/2}(2me)^{1/4}\, d$$

or

$$j = \left(\frac{2}{me}\right)^{1/2} \frac{V_B^{3/2}}{9\pi d^2}, \tag{12}$$

which is the Child-Langmuir $\frac{3}{2}$-power law for space-charge-limited current flow between two planes separated by a distance $d$ with a potential $V_B$ between them.

The top c[illegible]e of Fig. 2 represents the case of small $j$, when the space charge is small and the potential therefore a linear function of $x$. The middle curve shows the case when $j$ is at the value given in Eq. (12); then the electric field is zero at $A$ and a further increase in emission does not increase the current because no field acts on the particles at $A$.

If now the particles are allowed to have finite velocities when they are emitted, their inertia allows them to leave the surface $A$ even when no electric field is present. This has the effect of depressing the potential below zero and building up a field which opposes the emission of electrons. The potential curve then looks like the bottom curve in Fig. 2, with a potential minimum $V_m$ at $x = x_m$. In the case of a Maxwellian distribution of emitted electrons, the potential distribution can be found by integrating over the initial distribution of temperature $kT$. To first order in $\eta^{-1/2}$, where $\eta = eV/kT$, Langmuir (*1*, p. 379) finds for the space-charge-limited current

$$j = \left(\frac{2}{me}\right)^{1/2} \frac{1}{9\pi} \frac{(V - V_m)^{3/2}}{(d - x_m)^2} \left(1 + \frac{2.66}{\sqrt{\eta}}\right). \tag{13}$$

This shows clearly the increase of current due to finite temperature. The values of $V_m$ and $x_m$ in Eq. (13) must be found by a more complicated procedure, but for practical purposes they are small and may be neglected. Although we have for definiteness specified electrons, the Child-Langmuir law obviously holds also for ions if the appropriate mass and temperature are used.

### 2.3 The Sheath Criterion

Let us now introduce a second species of charged particle, so that we have a species 1 which is accelerated from $A$ to $B$ and a species 2 of equal and opposite charge which is repelled from $B$. We want eventually to identify surface $A$ with the surface of the plasma and $B$ with the surface of a wall or probe. Since a plasma is very nearly neutral (by definition), we require that $n_1 \approx n_2$ at $A$.

Our purpose in treating this problem is to gain some physical insight into the limitations of the approximation of a definite sheath edge which separates the plasma region, in which there are no electric fields, from the sheath region, in which large fields can exist. If the plane $A$ in Fig. 2 is to represent the sheath edge, then to ensure a smooth transition to the plasma solution, the electric field of the sheath and its derivatives must nearly vanish there. We shall find that this condition imposes a requirement on the velocity distribution of the particles emitted at $A$ and collected at $B$.



For simplicity, we shall treat first the somewhat degenerate case in which $T_1 = 0$, i.e., the accelerated particles have no random motion. In this case we must give them a nonvanishing drift velocity $v_0$ at $A$, since otherwise their velocity at $A$ would be 0 and their density infinite if their current is to be finite.

Since there can be no particles of type 1 traveling from $B$ to $A$, the distribution function of 1 is

$$\begin{aligned} f_1(0, v) &= n_0 \delta(v - v_0), \qquad v_0 > 0 \\ f_1(x, v) &= n_0 \delta \left[\left(v^2 + \frac{2q_1 V}{m_1}\right)^{1/2} - v_0\right]. \end{aligned} \tag{14}$$

We now assume that the potential $B$ is so large that almost all particles 2 are repelled; their distribution will then be Maxwellian:

$$f_2(x, v) = n_0 \left(\frac{m_2}{2\pi k T_2}\right)^{1/2} \exp\left[-m_2\left(v^2 + \frac{2q_2 V}{m_2}\right)/2kT_2\right]. \tag{15}$$

With the dimensionless variables

$$\eta = -\frac{q_1 V}{kT_2}, \qquad u = v\left(\frac{m_1}{2kT^2}\right)^{1/2}, \qquad \xi = x\left(\frac{4\pi n_0 q_1^2}{kT_2}\right)^{1/2}, \tag{16}$$

this becomes

$$f_2(\eta, u) = n_0 \left(\frac{m_2}{\pi m_1}\right)^{1/2} \frac{1}{v_s} \exp\left(-\frac{m_2}{m_1} u^2 - \eta\right), \tag{17}$$

where we have set $q_1 = -q_2$, and where $v_s = (2kT_2/m_1)^{1/2}$. Note that since particles 1 are accelerated, $q_1 V$ is always negative, and therefore $\eta$ always positive. Similarly, Eq. (14) becomes

$$f_1(\eta, u) = n_0 v_s^{-1} \delta[(u^2 - \eta)^{1/2} - u_0]. \tag{18}$$

The densities are found by integrating with respect to $v_s\, du$:

$$\begin{aligned} n_2 &= n_0 e^{-\eta} \\ n_1 &= n_0 \int \delta(y - u_0) \frac{y\, dy}{(y^2 + \eta)^{1/2}} = n_0(1 + \eta u_0^{-2})^{-1/2}. \end{aligned} \tag{19}$$

Poisson's equation is then

$$\eta'' = n_0[(1 + \eta u_0^{-2})^{-1/2} - e^{-\eta}]. \tag{20}$$

With the use of the integrating factor $\eta'$, the integral from 0 to $x$ is

$$\tfrac{1}{2}\eta'^2 = n_0\{2u_0^2[(1+\eta u_0^{-2})^{1/2}-1]+e^{-\eta}-1\}+\tfrac{1}{2}\eta_0'^2. \tag{21}$$

For the moment, let us neglect $\eta_0'$. The left-hand side in Eq. (21) must be positive; hence

$$2u_0^2[(1+\eta u_0^{-2})^{1/2}-1] > 1-e^{-\eta}. \tag{22}$$

Near the origin $\eta = 0$, this inequality becomes, upon expanding,

$$2u_0^2[\tfrac{1}{2}\eta u_0^{-2}-\tfrac{1}{8}\eta^2u_0^{-4}] > \eta-\tfrac{1}{2}\eta^2$$

$$u_0 = \left(\frac{m_1v_0^2}{2kT_2}\right)^{1/2} > \frac{1}{\sqrt{2}}. \tag{23}$$

This is the original sheath criterion derived by Langmuir (*2*, p. 140) and Bohm (*3*, Chapter 3). It states that in order for the sheath equation to have a solution for small $\eta$ there is a restriction on the streaming velocity assumed for particles 1 at plane $A$: namely, that it be larger than $(kT_2/m_1)^{1/2}$.

The most common application of this criterion is in the case of ion collection, in which ions are particles 1 and electrons particles 2. In many discharges the ion temperature is much lower than the electron temperature, so that the assumption $T_1 = 0$ is applicable. Equation (23) then says that the ions must stream into the sheath boundary with an energy greater than $\frac{1}{2}kT_e$, which is much larger than their thermal energy.

The reason for this restriction on the cold species can be seen by plotting the density, as given by (19), logarithmically against potential $\eta$, as shown in Fig. 3. The trapped particles 2 have a density which appears as a straight line on the semilog plot. If $\eta''$ is rigorously zero, the curve for $n_1$ starts at the same point $n_0$ as does $n_2$, and its initial slope depends on $u_0$. If $u_0$ is small, $n_1$ is less than $n_2$ for small $\eta$. Referring to Poisson's equation,

$$n_0\eta'' = n_1 - n_2,$$

we see that if $\eta_0' = 0$ and $\eta$ is to be positive, $\eta''$ must be positive near $\eta = 0$. If $u_0$ is too small, $\eta''$ is negative, and this will not permit a monotonic solution for $\eta(\xi)$. The solution will oscillate between two values of $\eta$, corresponding to an imaginary value of $\eta'^2$. If $u_0$ were large, we see from Fig. 3 that $n_1$ is always larger than $n_2$, and the problem does not arise. The critical condition is that

$$\left(\frac{dn_1}{d\eta}\right)_0 = \left(\frac{dn_2}{d\eta}\right)_0. \tag{24}$$

From Eq. (19), this is just

$$-\frac{n_0}{2}u_0^{-2} = -n_0, \qquad \text{or} \qquad u_0^2 = \tfrac{1}{2},$$

the same condition as Eq. (23). This equivalence was first pointed out by Allen and Thonemann (*4*).

The proof given above is subject to the criticism that $\eta$, $\eta'$, and $\eta''$ cannot all vanish at $x = 0$, since then only the trivial solution is possible. In practice $\eta_0'$ and $\eta_0''$ have small but finite values. If $\eta''$ is positive, for example, then by Eq. (20) $n_1$ must exceed $n_2$ at $x = 0$, as is illustrated by the dotted line in Fig. 3. The curve $n_1(\eta)$ may then dip below $n_2$, and the critical value of $u_0$ is reduced. This effect, however, is slight as long as the Debye length is small compared to the characteristic lengths in the plasma, such as the mean free path or an ionization length. The effect of finite $\eta_0'$ and $\eta_0''$ has been computed by Ecker and McClure (*5*).

If now the accelerated particles are allowed to have a spread in energy at the sheath edge, the critical drift velocity $u_0$ given by Eq. (23) is considerably reduced; however, the value of $u_0$ then cannot be expressed simply, even for a Maxwellian distribution.



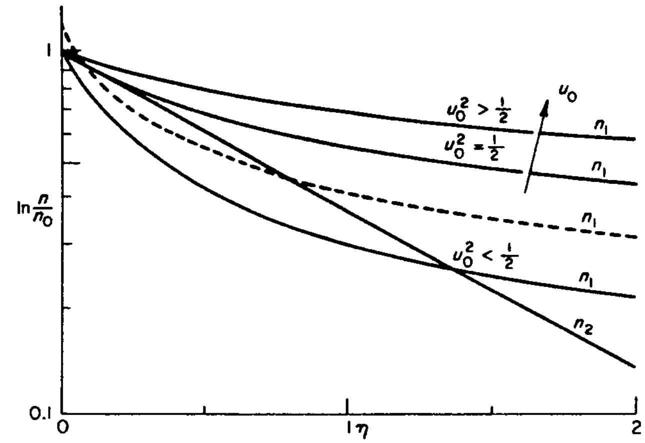


FIG. 3. Schematic of ion density ($n_1$) and electron density ($n_2$) distributions in a sheath as a function of potential $\eta$, for various values of incident velocity $u_0$ of the cold ions.

We may point out the implications of the sheath criterion on the probe characteristic of Fig. 1. Consider the usual case in which $T_i \ll T_e$. Then in part $A$ of the characteristic, where electrons are accelerated toward the probe, the sheath criterion (23) tells us that the electrons must enter the sheath with a drift velocity greater than $(kT_i/m)^{1/2}$. Since this is small compared to the random electron velocity, and the finite electron temperature makes the criterion even less severe, the current entering the sheath is closely approximated by the random electron current in the plasma. Use is made of this in Section 3.1. On the other hand, in part $C$ of the characteristic, where ions are accelerated to the probe, the sheath criterion requires the ions to have a directed velocity greater than $(kT_e/M)^{1/2}$, which is much larger than the random velocity. The velocity distribution at the sheath edge is then unknown and the ion current must be computed laboriously, as is done in Sec. 3.3. However, for sheaths thin compared to the probe radius, so that the geometry is almost planar, it will turn out that the ion current density is given roughly by $n_0$ times this critical velocity. This is essentially the reason probes are insensitive to ion temperature. The situation is, of course, reversed if $T_i$ is much larger than $T_e$.

We have, for purposes of illustration, considered the case of an infinite plane probe, but it is clear that such a probe cannot actually exist, since in the absence of ionization all the plasma would eventually be lost to the probe. The probe current in steady state is given by the rate of ionization in the plasma, and therefore the probe is in a sense actually an electrode. As we shall see in Section 3.3, the situation is different in the case of spherical or cylindrical probes, for which the probe current depends only on the properties of the plasma far from the probe and not on the mechanism which produces the plasma. However, except for geometrical factors, the basic prediction of the plane sheath criterion is still valid; that is, the shielding of the probe by the sheath is incomplete, and a total potential drop of order of magnitude $kT_2$ must exist in the plasma region to accelerate particles 1 to this energy by the time they reach the point near the boundary where the quasi-neutral assumption fails.

Further discussion of plane sheaths, which necessarily involves the ionization mechanism, may be found in the work of L. Tonks and Langmuir (*2*, p. 176). The particularly simple case of no collisions has been treated by Harrison and Thompson (*6*), Auer (*7*), and Self (*8*). A rigorous boundary-layer analysis of the plasma-sheath transition has been given by Caruso and Cavaliere (*9*). The stability of the ion stream in this case has been examined by Chen (*10*). The effect of a weak magnetic field on the sheath criterion has been studied by Allen and Magistrelli (*11*).

## 3 Probe Theory in the Absence of Collisions and Magnetic Fields

The exact way in which the plasma parameters are related to the probe characteristic will depend on the shape of the probe and the relative magnitudes of the collision length, the probe dimensions, the Debye length, the Larmor radius, and so forth. In this section we shall discuss the simplest case—that in which both collisions and magnetic fields are negligible. This case is essentially that covered by the original theory of Langmuir. There is, however, one exception; that is, in dealing with saturation ion current the effect of acceleration of ions in the plasma region (which we discussed in connection with the sheath criterion) was at first unknown to Langmuir. For the proper treatment of ion saturation current we shall have to turn to comparatively recent work. We shall confine ourselves to plasmas consisting of singly charged positive ions and electrons. Extensions of the theory to include negative ions or multiply charged ions is straightforward. The main difference from the discussion of Sec. 2.3 is that now we shall have to consider particle orbits in more than one dimension.

### 3.1 Probe Current in a Prescribed Electric Field

We now turn to the problem of sheath formation on actual probes, which are normally not planar but cylindrical or spherical, since such shapes do not disturb the plasma as much as a large flat surface. Particles can now move in orbits in a central force field, and the density is no longer a simple function of potential as it was in the one-dimensional case. Again we have Poisson's equation

$$\nabla^2 V = -4\pi(q_1 n_1 + q_2 n_2),$$

but now not only is the Laplacian more complicated but also $n_1$ is a complicated integral involving $V$. The solution for $V$ must even in the simplest case be found numerically. However, in some physical situations the probe current can be found without knowing the exact behavior of $V(r)$. In these situations the original theory of Langmuir is applicable. In describing this theory we shall assume that the function $V(r)$ is already known.

#### 3.1.1 *Thin Sheath: Space Charge Limited Current*

Suppose that the prescribed electric field is such that the potential drop around a charged spherical or cylindrical probe attracting particles of type 1 is concentrated in a thin layer of radius $s$ surrounding the